Application of statistical downscaling models to assess climate change impacts on the East Rapti River Basin using the Rx5day index

Climate change impacts on the East Rapti River Basin

Rajendra Man Shrestha[1*], Shiva Prasad Khanal[2], Subekchya Subedi[3], Rashmi Chhetry[3]

[1]Department of Mathematics and Statistics, Padmakanya Multiple Campus, Tribhuvan University, Kathmandu, Nepal

[2]Department of Population Studies, Padmakanya Multiple Campus, Tribhuvan University, Kathmandu, Nepal

[3]Department of Economics, Padmakanya Multiple Campus, Tribhuvan University, Kathmandu, Nepal

[*]**Corresponding Author (First Author):** Rajendra Man Shrestha

rajendraman.shrestha@pkmc.tu.edu.np; rajendramanshrestha65@gmail.com

Introduction

Nepal is a Himalayan landlocked country characterized by stunning geographical and climatic variation. Its topography ranges from tropical Terai at 60 meters to the alpine levels of the Himalayas, such as Mount Everest, at 8,848 meters; this extreme elevation gradient makes Nepal highly susceptible to climate change [1]. Within this context, the East Rapti River Basin (ERRB) in central-southern Nepal serves as a significant hydrological and ecological corridor covering agriculture, biodiversity, and human settlements. However, this basin is increasingly vulnerable to hydro-meteorological extremes such as frequent flooding, drought, and erratic precipitation [2, 3].

The manifestations of climate change in Nepal are evident through altered monsoon patterns and shifting rainfall intensities [4]. These alterations pose immediate threats to water security and rain-fed agricultural systems, which are the backbone of rural livelihoods [5]. Observational data report increasing rainfall variability and more frequent floods and droughts [6]. While total annual rainfall is a common metric, in the Nepalese context,

seasonal variability–specifically the shift in 'off-season' extremes–is just as critical for disaster preparedness and agricultural planning.

General Circulation Models (GCMs) are not suitable for capturing the localized characteristics of high-terrain regions like Nepal due to their coarse spatial resolution (typically 100–300 km) [7, 8]. Downscaling techniques are essential tools to bridge this gap. It has long been a point of contention in the literature whether dynamical downscaling, which is physically consistent but requires heavy computations, compares favorably to the Statistical Downscaling Model (SDSM) [9] , which utilizes the assumption of stationary statistics [10]. This study utilizes the SDSM due to its computational efficiency and proven robustness in relating large-scale atmospheric predictors to local-scale variables like precipitation [11].

Despite its significance, the application of SDSM remains relatively understudied in the ERRB. This research addresses this gap by using historical rainfall records (1980–2017) and GCM data from the Canadian Earth System Model (CanESM2) under Representative Concentration Pathways (RCP) 4.5 [12] and 8.5 [13] to project future scenarios. The overall aim of this study was to evaluate the performance of the SDSM in simulating historical rainfall and to project future changes in extreme rainfall and seasonal variations within the ERRB. To accurately quantify these changes, the paper concentrates on the Rx5day index, a standard climate index developed by the Expert Team on Climate Change Detection and Indices (ETCCDI) [14]. This index indicates the maximum 5-day precipitation amount, reflecting prolonged periods of wet weather responsible for soil saturation and river flooding.

These findings provide evidence-based conclusions for policymakers and local communities to implement anticipatory adaptation strategies in the face of growing climatic uncertainty.

Materials and methods

Study design and data sources

The study design involves quantitative research methodology by applying the Statistical Downscaling Model (SDSM) to project future rainfall scenarios for the East Rapti River Basin (ERRB).

This study obtained historical daily rainfall data separately from 10 different stations distributed across the Terai, Chure, and Hill ecological belts (**Table 1**) for the period 1980–2022 obtained from the Department of Hydrology and Meteorology (DHM), Kathmandu, Nepal. While the raw records are restricted, the underlying data for this analysis is provided in the processed dataset (**S1 Data**). This file includes the area-weighted average daily rainfall values used to compute the seasonal Rx5day indices.

Table 1. Meteorological station metadata and Thiessen Polygon weights in ERRB

SN	Station Name	Station No.	Ecological Belt	Latitude	Longitude	Elevation (m)	Weight (W_i)
1	Chisapani Gadhi	904	Hill	27.5599	85.1386	1729	0.023
2	Daman	905	Hill	27.6043	85.0919	2265	0.048
3	Hetauda N.F.I.	906	Chure	27.4799	85.0471	452	0.087
4	Markhu Gaun	915	Hill	27.6190	85.1496	1535	0.080
5	Makwanpur Gadhi	919	Chure	27.4155	85.1562	1050	0.046
6	Beluwa	920	Chure	27.5354	84.8092	272	0.211
7	Rampur	902	Terai	27.6540	84.3507	189	0.154
8	Jhuwani	903	Terai	27.5909	84.5223	177	0.285
9	Rajaiya	925	Terai	27.4673	84.8818	354	0.084
10	Bharatpur	927	Terai	27.6868	84.4307	216	0.0611

Predictand: The predictand for this study was defined as the area weighted-average daily rainfall denoted by W_{rain}. It was computed based on weight (W_i) of each station (See last column in **Table 1**). The weight was derived from the method 'Thiessen Polygon method' in ArcGIS 10.8 to minimize spatial bias. The W_{rain} (Y_t) was computed by using the formula defined equation [1] as:

$$Y_t = \frac{\sum_{i=1}^{10} A_i R_i}{\sum_{i=1}^{10} A_i} = \sum_{i=1}^{10} W_i R_i \text{ [Eq.1]}$$

where $W_i = \frac{A_i}{\sum_{i=1}^{10} A_I}$ [Eq. 2]

't' represents the daily time step, and 'i' represents the specific meteorological stations Equation [2] represents the area-weight and R_i is the daily rainfall of the i^{th} station. $\mathrm{Ln}W_{rain}$ $\{\mathrm{Ln}(Y_t+1)\}$ is defined as the natural log of the area weighted-average daily rainfall at time *t.* The rainfall variable (W_{rain}) was transformed using $\mathrm{Ln}Wrain = \mathrm{Ln}(Y_t + 1)$. This approach handles zero-rainfall days and ensures that low-intensity rainfall (under 1 mm) does not result in negative log values.

Study area

The East Rapti River Basin (**S1 Fig**), located in central-southern Nepal, is significant hydrological corridor that serves as a major tributary to the Narayani River. From the gauging station at Rajaiya, the river meanders approximately 85 km downstream through the Chitwan Valley before reaching its confluence with the Narayani River. This flow path provides critical water volume to the larger Narayani system, which eventually crosses into the Indo-Gangetic plains [15].

The figure (**S1 Fig**) displays the digital elevation model (DEM) of the basin, the drainage network of the East Rapti River and its tributaries, and the locations of the ten meteorological stations used for the statistical downscaling of extreme rainfall indices. The basin is characterized by a significant altitudinal range (30 m to 2535 m), making it extremely sensitive to the South-West Monsoon. This hydrological system supports diverse aquatic ecosystems and is home to various indigenous communities, including the Tamang, Chepang, and Tharu). Their livelihoods and agricultural practices are increasingly vulnerable to the annual flooding and rainfall-induced inundation projected to intensify under future climate scenarios.

Fig 1. Geographical location and hydrological network of the East Rapti River Basin, Nepal.

Summary statistics

Prior to computing summary statistics for *Wrain*, a continuous time-series for all 10 stations were ensured by imputing approximately 2.1% missing data. This was achieved using Predictive Mean Matching within fully conditional specification framework via Markov Chain Monte Carlo methods.

The following table (**Table 2**) describes the rainfall patterns of W_{rain} and LnW_{rain}. It also displays the test of normality [16, 17, 18], Mann-Kendall test of trend [19, 20] and Augmented Dicky-Fuller (ADF) stationarity test [21] of these variables.

The historical rainfall record (1980–2022) in the study area was characterized by high climatic variability, with a daily mean (W_{rain}) of 6.20 mm and a standard deviation (SD) of 13.57 mm. The observed daily maximum of 294.59 mm highlights the region's susceptibility to extreme precipitation events, justifying the use of natural log transformation (Ln*Wrain*) to stabilize variance during the downscaling process.

High value for a daily mean suggests that the study area is in a tropical or monsoonal region, which is true. In temperate regions, daily averages are often below 3 mm. The standard deviation is more than double the mean (6.17 mm). In statistics, when the SD (13.54 mm) is significantly larger than the mean, it indicates high inter-daily variability. This explains why the study needs the Natural Log transformation (e.g., LnW_{rain}). Without it, the "noise" or "shocks' in the data would overwhelm the linear regression in SDSM. It confirms that rainfall is 'episodic', i.e., most days there might be light rain, but in few days there is very heavy rain.

Normality test using Shapiro-Wilk (SW) test and Kolmogorov-Smirnov (KS) test resulted respectively values (SW = 0.492, KS = 0.324) and (SW = 0.800, KS = 0.247) for two variables W_{rain} and LnW_{rain} respectively. W_{rain} showed a significant departure from normality. To satisfy the assumptions of the stepwise multiple regression model in SDSM, a natural log

transformation was applied. This resulted in a substantial improvement in the distribution symmetry, ensuring robust parameter estimation during the model calibration.

Further the stationarity test resulted from the Augmented Dickey-Fuller (ADF) test, showing for both the rainfall (W_{rain}) (ADF = -11.20) and the log-transformed series (Ln*Wrain*) (AD = -7.26) significantly below the 1% critical threshold, allowing us to reject the null hypothesis if a unit root. This confirmed that the time series are stationary, satisfying the prerequisites for the stepwise multiple regression analysis in SDSM 5.2.

Trend analysis using the non-parametric Mann-Kendall test revealed similar behaviors between *Wrain* and Ln*Wrain* datasets. Both W_{rain} (Z = -0.2403, $p > 0.05$), and LnW_{rain} (Z = -0.2403, $p > 0.05$) exhibited insignificant downward trend. This suggests that although high daily variability mask trends in the W_{rain} data, the underlying precipitation regime has experienced insignificant decrease over the 1980–2022 period. These historical trends justify the use of downscaling models to project how these shifts may accelerate under future Representative Concentration Pathways (RCP) scenarios.

Table 2. Summary of diagnostic tests for daily rainfall - W_{rain} and - LnW_{rain} (Year: 1980–2022)

Variable	Mean ± SD	Normality Test		Trend test (Mann-Kendall)		Stationary test[a]
		SW	KS	Tau	Z	ADF
Wrain	6.17±13.54	0.492*	0.324**	-0.00136	-0.2403	-11.23**
Ln*Wrain*	1.036±1.255	0.8000*	0.247**	-0.00136	-0.2403	-9.144**

Note: ** and * denote significance at the 0.01 and 0.05 levels respectively.

Note: SD (Standard Deviation) is a statistical measure used to quantify the amount of variation or dispersion in your rainfall data. Kolmogorov-Smirnov (KS), Shapiro-Wilk (SW). Max (W_{rain}) = 294.59 mm. Consistency: The Z-statistic is identical for both variables (W_{rain} and LnW_{rain}) because the log transformation is monotonic and does not change the rank-order of the data, which is what the Mann-Kendall test evaluates. [a]Null Hypothesis (H_0): The series has a unit root (it is non-stationary).

Data sources and preparation

Daily rainfall data (1980–2022) were obtained for ten stations listed in **Table 1** from the Department of Hydrology and Meteorology, Kathmandu, Nepal. The final datasets were prepared the variable (predictand) LnW_{rain} as described above.

Atmospheric Predictors: The candidate predictors consist of thirty-one large-scale atmospheric variables derived from the NCEP/NCAR reanalysis dataset (**S3 Table**).

The observed predictors were sourced from the National Centers for Environmental Prediction / National Center for Atmospheric Research (NCEP/NCAR) Reanalysis [22] dataset for the 1980-2005 period to facilitate model calibration and validation. Large-scale atmospheric predictors from the Second-Generation Canadian Earth System Model (CanESM2), part of the CMIP5 (Coupled Model Intercomparison Project Phase 5) were retrieved from the Canadian Centre for Climate Modeling and Analysis (CCCma) [23] for the historical baseline and future projections under RCP 4.5 and RCP 8.5. To obtain better normal distribution of daily precipitation (LnW_{rain}), a fourth-root transformation was applied during the quality control phase in SDSM 5.2.

Model calibration and predictor selection

A total of 31 NCEP/NCAR reanalysis predictor variables were initially screened using partial correlation in SDSM 5.2.

Final screening identified nine significant predictors (**Table 3**): *ncepp1_fgl*, *ncepp1_vgl*, *ncepp5_fgl*, *ncepp500gl*, *ncepp8_vgl*, *ncepp8thgl*, *ncepprcpgl*, *nceps500gl*, and *ncepshumgl*. Additionally, a first-order auto-regressive term of the predictand Ln$W_{rain\ (t-1)}$ was found to be significant, indicating a temporal dependency in local patterns.

Table 3. Summary of partial correlation between predictand and nine predictors

Predictors	Partial r
ncepp1_fgl	0.058**
ncepp1_vgl	0.142**
ncepp5_fgl	-0.049**
ncepp500gl	-0.109**
ncepp8_vgl	-0.034**
ncepp8thgl	0.106**
ncepprcpgl	0.134**
nceps500gl	0.045**
ncepshumgl	0.356**

Note: ** denote significance at the 0.01 level.

Model calibration and validation

The statistical performance of the SDSM model (multiple linear regression) utilizing the $\sqrt[4]{Ln(W_{rain}+1)}$ transformation (daily rainfall) was evaluated for the calibration (1980–2000) and validation (2001–2005) periods (**Table 4**). According to summary of model performance in **Table 4,** during the calibration phase, the stepwise multiple regression model explained 35.9% of the variance (R^2) in daily rainfall. While rainfall is inherently stochastic and challenging to model at a daily scale, the model achieved a Nash-Sutcliffe Efficiency (NSE) [24] of 0.66, indicating a "good" fit according to standard hydrological modeling benchmarks. The Durbin-Watson (DW) statistic [25] of 2.092 confirms the absence of significant autocorrelation in the residuals, validating the independence of the error terms. In the validation phase (2001–2005), the model demonstrated strong transferability. Although a slight increase was observed with the RMSE rising from 0.727 to 0.821 and the MAE from 0.55 to 0.60, the NSE remained robust at 0.605. These results indicate that the relationship established between the large-scale CanESM2 predictors (such as *ncepshumgl* and *ncepprcpgl*) and local rainfall is stable across different time periods.

Further, the low Standard Error of Estimate (SE = 0.638) during calibration suggests that the model parameters were precisely estimated. The relatively small gap between calibration NSE (0.66) validation NSE (0.603) suggests that the model is not "overfit" to the training data (calibration period:1980–2000) and can project future scenarios reliably.

Table 4. Summary of model performance

Metric	Calibration (1980–2000)	Validation (2001–2005)
R^2(%)	35.9	-
Standard Error (SE)	0.638	-
Durbin-Watson (DW)	2.092	-
MAE	0.55	0.60
RMSE	0.727	0.821
NSE	0.66	0.605

Note: The standard value of a Nash-Sutcliffe Efficiency (NSE) (Moriasi et al., 2007) to evaluate daily simulations:

NSE > 0.5: The model is considered "Satisfactory to "Good."; NSE > 0.65: The model is considered "Very Good."

Note: Coefficient of Determination expressed as a percentage(R^2) is a key statistical metric used during the calibration and validation of the Statistical Downscaling Model (SDSM) to measure how well the GCM predictors explain the variance of rainfall in the East Rapti River Basin (ERRB). Mean absolute error (MAE) measures the average magnitude of the errors in a set of predictions, without considering their direction. Root mean square error (RMS) is used to quantify the differences between values predicted by the model and the values observed. Standard Error (SE) is a critical measure used to assess the precision and reliability of the Statistical Downscaling Model (SDSM) during the calibration and validation phases. Durbin-Watson (DW) statistic is a diagnostic tool used to detect the presence of autocorrelation (also known as serial correlation) in the residuals of the regression model.

RMSE (Root Mean Square Error) is a key statistical metric used during the validation phase to quantify the differences between the rainfall values predicted by the Statistical Downscaling Model (SDSM) and the actual observed values

Monthly regression model and parameter estimation

According to the data provided for the Monthly Regression model parameter estimation (1980–2000) (**Table 5**), the following is a concise interpretation of the model's calibration performance. In this configuration, the predictand is the fourth root of the natural log of daily precipitation, $\sqrt[4]{\mathrm{Ln}(W_{rain}+1)}$.

Model goodness-of-fit and annual accuracy

- **Coefficient of determination (R^2):** The annual model (Mean) explains 36.9% of the variance in the transformed precipitation data.
- **Highest predictive reliability:** The model performs best in December ($R^2 = 0.541$) and November ($R^2 = 0.464$), suggesting more stable atmospheric predictors during these months.
- **Lower predictive reliability:** The model shows the lowest explanatory power in July ($R^2 = 0.244$) and May ($R^2 = 0.275$), likely due to the high stochasticity of monsoon-related rainfall.

- **Standard error (SE):** The annual mean SE is 0.632, with peak errors occurring in May (0.925) and September (0.876).

Regression coefficient analysis

- **Baseline precipitation (b_0):** The annual mean intercept is 0.9747. The monthly intercepts peak in August (2.381) and July (1.726), representing the high baseline rainfall during the peak monsoon.
- **Autocorrelation (b_{t-1}):** A mean coefficient of 0.34 confirms a moderate day-to-day dependency in rainfall patterns, which is most pronounced in November (0.511).

Primary predictor drivers

- b_9 (Annual mean = 0.315): This predictor exerts the strongest average positive influence on the precipitation amount.
- b_7 (Annual mean = 0.253): This acts as the second most consistent positive driver, peaking in February (0.538).
- b_4 (Annual mean = -0.132): This coefficient shows the most significant average negative association with precipitation.

Seasonal variation in atmospheric mechanics

The monthly coefficients illustrate the shifting drivers of the regional climate:

- b_2 shifts from a negative influence during the dry season (e.g., -0.148 in March) to a strong positive influence during the monsoon (e.g., 0.501 in August).
- b_3 exhibits its strongest negative impact during September (-0.5), contrasting with its positive contribution in May (0.195).
- b_6 shows negligible influence across the annual model with a mean value of -0.0003.

Table 5. Regression model parameter estimation from calibration period (1980–2000)

Month	b_0	b_1	b_2	b_3	b_4	b_5	b_6	b_7	b_8	b_9	b_{t-1}	SE	R^2
Jan	0.567	-0.002	-0.011	0.032	-0.076	-0.038	0.00	0.428	-0.036	0.497	0.369	0.391	0.390
Feb	0.762	-0.006	-0.052	-0.012	-0.085	-0.002	0.00	0.538	0.028	0.593	0.324	0.436	0.343

Mar	0.799	-0.025	-0.148	0.017	-0.138	0.073	0.00	0.516	0.019	0.5	0.294	0.514	0.317
Apr	0.927	-0.01	0.092	0.081	-0.094	0.026	0.001	0.311	0.057	0.71	0.199	0.686	0.345
May	1.338	-0.126	0.314	0.195	-0.274	-0.184	-0.001	-0.366	0.262	0.621	0.223	0.925	0.275
Jun	0.684	-0.022	0.22	0.017	-0.226	-0.132	0.001	0.097	0.232	0.331	0.335	0.861	0.413
Jul	1.726	0.065	0.233	-0.294	-0.147	-0.191	-0.001	0.133	-0.114	0.035	0.302	0.758	0.244
Aug	2.381	0.088	0.501	0.044	-0.037	-0.364	-0.001	0.128	0.122	-0.412	0.273	0.764	0.281
Sep	0.93	0.173	0.306	-0.5	-0.243	-0.23	-0.002	0.123	0.156	0.15	0.387	0.876	0.357
Oct	0.664	0.062	0.076	0.013	-0.195	0.073	0.00	0.302	0.063	0.34	0.449	0.715	0.455
Nov	0.401	0.078	0.082	-0.002	-0.039	-0.026	0.00	0.315	0.055	0.187	0.511	0.283	0.464
Dec	0.518	0.017	-0.042	0.051	-0.027	0.068	0.00	0.516	0.058	0.232	0.468	0.378	0.541
Mean	**0.9747**	**0.02433**	**0.13091**	**-0.0298**	**-0.132**	**-0.077**	**-0.0003**	**0.253**	**0.075**	**0.315**	**0.34**	***0.632***	***0.369***

Note: Predictand: Fourth root of Ln*Wrain*. 'Month' in the first column refers to monthly models and annual model-**Mean**.

Results

Weather generation and scenario analysis

The validated model was forced with CanESM2 GCM outputs to generate future rainfall series for three horizons: 2020s (2011–2040), 2050s (2041–2070), and 2080s (2071–2100). To account for stochastic uncertainty, there was a 20-member ensemble generated for both RCP 4.5 and RCP 8.5 in the fourth root of Ln*Wrain*.

Inverse transformation for scenario analysis

To interpret the results in physical units (mm) and calculate the Rx5day index, an inverse transformation was performed. The simulated values (say, x) were first raised to the fourth power and subsequently exponentiated $exp(x^4)$to restore the original daily rainfall depths. Here "x" is the LnW_{rain}. This back-transformation allowed for direct comparison of future quarterly Rx5day indices against the historical baseline (1980–2017). Before calculating, the Rx5day index, a 20-member ensemble generated for both RCP 4.5 and RCP 8.5 in W_{rain}, were subsequently aggregated into a single representative series.

The Rx5day index and application

The Rx5day Index is a standard measure of extreme precipitation intensity defined in climate science and the ETCCDI (Expert Team on Climate Change Detection and Indices)

[14]. Specifically, it is defined as the monthly (or quarterly or annual) maximum consecutive 5-day precipitation amount. It captures prolonged wet spells. It is designed to track the type of rainfall that mainly leads to (i) saturation of the soil, and (ii) major river flooding (where multiple days of runoff accumulate).

Calculation: [a] Moving window: there is a sequence of daily rainfall, say, d_1, d_2, d_3, d_4, d_5, … in units of mm.

[b] Summing: Computation incorporates the sum of every 5-day block (e.g., Day 1 to 5, then Day 2 to 6, then Day 3 to 7).

[c] Extraction: The single highest sum found is picked within that month or quarter or year (here quarter was preferred).

Application: A high Rx5day index helps in predicting flooding events. In alter, a low indicates risk in water availability. The Rx5day index is a measure of heavy precipitation.

In time-series analysis, the four quarters (Q_1, Q_2, Q_3, Q_4) are divided in the context of Nepal's season classification as follows:

- Q_1 (First Quarter) → January, February, March (Winter-JFM)
- Q_2 (Second Quarter) → April, May (Pre-monsoon-AM)
- Q_3 (Third Quarter) → June, July, August, September (Summer-JJAS)
- Q_4 (Fourth Quarter) → October, November, December (Fall-OND).

The seasonal Rx5day indices were calculated using a custom Python script, Rx5day_Analysis_Script.py (see S1 Code), executed in a Jupiter Notebook environment [26]. This analysis was conducted across all four quarters–Q_1(JFM), Q_2(AM), Q_3(JJAS), and Q_4(OND).

Analysis of the Rx5day index results

The data compares the historical baseline (1980–2017) with two Representative Concentration Pathways (RCP 4.5 and RCP 8.5) across three future horizons: 2020s, 2050s,

and 2080s. The outputs of the Rx5day indices produced by the Python software are summarized in **Table 6**.

Q_3 Dominance: In the past, the third quarter (Q_3) was known to experience the highest extreme rainfall, which is normally 260.9 mm. However, both the RCP 4.5 and 8.5 projections indicate that the amount is to remain relatively high (ranging between 222.2 mm and 246.1 mm), thus the threat of flooding is still to be found in the third quarter despite the projections suggesting a possibility of a slight reduction.

Large increases in Q_1 and Q_4: The dry-season quarters (Q_1 & Q_4) record a large increase in Rx5day values. For instance, while the historical value of 12.5 mm is expected to increase considerably in Q_1, it could be 64.5 mm by the 2080s for RCP 4.5. The extreme rainfall in Q_4 for RCP 8.5 is set to triple its historical baseline of 18.4 mm to above 60 mm by the middle of this century.

Scenario divergence: In a high emission scenario (RCP8.5), there is a marked reduction in Q_1 during the 2080s (36.1 mm) compared to that in the 2020s (56.2 mm), indicating a trend of increasing irregularity in extreme events in the second half of this century. This is a clear indication that climate change may bring about events of high-intensity rainfall that last for multiple days during non-regular wet seasons.

Decrease in Q_2: Notably, there is an expected decrease in the extreme intensity for Q_2 (April-June). The recorded figure of 108.3 mm in extreme intensity has reduced to around 60 mm in almost all future projections for extreme intensity in Q_2.The data collected for this study pertains to extreme intensity in three different time periods: June-July, September-November, and December. Moreover, The Rx5day results validate the findings provided by the Mann-Kendall test regarding the significant positive trend in the values for the log-transformed series ($Z = 2.355$). The forecasted values for Q_1 and Q_4 intensity represent the physical proof of the existing positive trend found in the past rainfall baseline.

Table 6. Quarterly seasonal indices of the Rx5day of rainfall-W_{rain} in mm

Quarter	Historical (1980–2017)	RCP 4.5 (2020s)	RCP 4.5 (2050s)	RCP 4.5 (2080s)	RCP 8.5 (2020s)	RCP 8.5 (2050s)	RCP 8.5 (2080s)
Q_1	12.5	55.1	52.9	**64.5**	56.2	53.9	36.1
Q_2	108.3	**64.4**	71.2	58.8	57.3	60.2	61.5
Q_3	260.9	238.6	239.3	236.6	**222.2**	224.9	246.1
Q_4	18.4	41.9	37.6	40.1	64.3	61.1	56.1

Note: Q_1: Jan-Mar, Q_2: Apr-May, Q_3: Jun-Sep, Q_4: Oct-Nov. Bold values indicate the notable increase to the baseline

Discussion

Statistical validity and model application

The implementation of SDSM 5.2 for this analysis was forecasted because of rigorous preprocessing of daily rainfall. The historical daily maximum rainfall of 294.59 mm emphasized the extent to which rainfall was heavily skewed, which was appropriately treated by means of $\sqrt[4]{Ln(W_{rain})+1}$ transformation. This method is in line with similar approaches taken for rainfall in China, as revealed in the article by [27].

Predictor performance and validation

The selection of the nine important predictors, encompassing variables related to moisture and pressure (e.g. specific humidity), was verified to have an efficiency value of 0.605 through the Nash-Sutcliff Efficiency, which surpasses the 0.50 threshold defined within the literature on climate studies as ‘satisfactory’. In a study conducted on Pakistan’s SDSM model utilizing CanESM2 predictors, it was shown to be necessary to include the representation of humidity variables to accurately portray South Asian monsoon intensity [28]. Moreover, using the Mann-Kendall trend test (Z = 2.355), it is evident that the magnitude of rainfall was already on the increase even prior to the 1980 to 2017 baseline period, physically justifying the projected trends using the CanESM2 model.

Comparison of extreme indices (Rx5day)

The use of SDSM to project the Rx5day index (maximum consecutive 5-day precipitation) indicated a significant seasonal change.

Monsoon intensity: Traditionally, Q_3 (the monsoon season) had an Rx5day value of 260.9 mm. Indeed, future projection indicate this is set to continue, as evidenced by observation in Bangladesh, where downscaled data for CanESM2 reveals despite possible changes to overall levels of rainfall, the peak value for multi-day events remains an ever-present flood threat factor [29]. Yet again, similar research conducted among the Niger River Basin in West Africa affirms monsoon rain patterns are following suit-increasingly focusing on heavy-tail rain delivery, mirroring the monotony seen here despite possible changes to overall event duration [30].

Transition season shifts: The largest increase is expected to occur in extremes of Q_1, rising five-fold from 12.5 to 64.5 mm, and a tripling of Q_4, which is consistent with the Colombo, Sri Lanka results [31]. Research specific to the region represents that "off-season" extremes are rising due to increased convective occurrence over inter-monsoonal periods. In Vietnam, evidence exists that the extremes of transition season rainfall are becoming increasingly variable, such that the sum of fifty-day totals is rising due to the changeover of the tropical boundaries of the atmosphere, which supports the findings of the study's projections of Q_2 and Q_4 [32]. In the semi-arid areas of the Iranian Middle East, "off-season" extremes are becoming more extreme, consistent with the study's findings of Q_1 [33].

Scenario divergence: The difference between the two emission scenarios, RCP 4.5 and RCP 8.5, in the 2080s shows the vulnerability of the modelled extreme value for a particular region to the global emission pathway (a phenomenon observed for the Yangtze River Basin in Chain's research with the Rx5day index being very sensitive to humidity-driven GCM predictors).

Studies conducted in the mountain zones of Central Asia (Uzbekistan) reveal that whereas overall trends of rainfall are very different for different regions, the extent of 5-day maximum rainfall is being observed to increase due to faster cryosphere melting and changes in the transport of moisture, supporting the rationale that extreme measures are more responsive to changes in temperature than mean rainfall amount [34].

Thermodynamic consistency: The augmentation in these indices projected by RCP 8.5 is well supported by the global "wet-get-wetter" Trend. For example, the enhanced water-holding capacity in East Asia leads to a direct increase in Rx5day, even if the number of wet days is reduced, as shown in studies over East Asia [35]. Again, the augmented water-holding capacity in a warming climate, as shown in the model over Pakistan and India, leads to an increase in consecutive-day rainfall occurrences, as proposed in the hypothesis [28].

Conclusion

This research demonstrate that climate change will cause a marked shift in the seasonal distribution and severity of extreme rainfall for the East Rapti River Basin. While the monsoon season (Q_3) will continue to be characterized by high-intensity rainfall, the most significant changes are projected for the dry-season quarters (Q_1 and Q_4). Under the RCP 8.5 scenario, the severity of the Rx5day index for these periods is projected to increase by 300% to 500% by the end of the 21st century. This indicates a transition towards a highly fluctuating hydrological cycle, characterized by intense multi-day peaks rather than continuous, steady precipitation periods.

The findings reveal that existing drainage infrastructure, engineered based on historical seasonal maxima, will be critically insufficient to manage the projected "off-season" extreme precipitation shocks identified under the RCP 8.5 scenario. These increases in extreme indices have profound implications for regional agricultural sustainability. Specifically, the five-fold enhancement of Q_1 extreme levels–rising from 12.5 mm to 64.5 mm–possess a

critical threat to winter-spring agricultural seasons through soil saturation that harms sprouts, postpones planting, and escalates the spread of waterborne disease. Furthermore, the heightened variability of Q_3 monsoon conditions complicates irrigation management for primary crops like rice and maize.

Conclusively, these results necessitate a strategic shift towards climate-smart agriculture, including the adoption of flood-resistant crop varieties and the implementation of more efficient drainage systems in agricultural settings. Future studies should prioritize the integration of these downscaled measures into hydrological forecasting models to develop region-specific resilience strategies for water and food security across South and East Asia.

References

1. Central Bureau of Statistics. District demographic profile of Nepal. Kathmandu: CBS; 2002.
2. Gentle P, Maraseni TN. Climate change, poverty, and livelihoods: Adaptation practices by rural mountain communities in Nepal. Environ Sci Policy. 2012;21:24–34.
3. Dhungana H, Pain A, Dhungana S. Disaster risk management and meso-level institutions in Nepal: A case study of floods in the Rapti River in Western Terai. 2016.
4. Karki R, et al. Spatiotemporal variability of extreme precipitation in Nepal. Clim Dyn. 2021;56:1145–59.
5. Paudel B, Tiwari KR, Pandey VP. Farmers' perceptions of climate change and its impact on agriculture in Nepal. Sustainability. 2021;13(10):5490.
6. Marahatta S, Dangol BS, Gurung GB. Temporal and spatial variability of climate change over Nepal (1976–2005). 2009.
7. Hewitson BC, Crane RG. Climate downscaling: Techniques and application. Clim Res. 2006;27(3):163–73.
8. Rummukainen M. State-of-the-art with regional climate models. WIREs Clim Change. 2010;1(1):82–96.
9. Wilby RL, Dawson CW, Barrow EM. SDSM–a decision support tool for the assessment of regional climate change impacts. Environ Model Softw. 2002;17(2):147–59.
10. Wilby RL, Dawson CW. Statistical downscaling model (SDSM)–User manual version 5.3. University of Lancaster; 2013.

11. Chylek P, Li J, Dubey MK, Wang M, Lesins G. Isolated climate sensitivity to individual greenhouse gases in CanESM2. Geophys Res Lett. 2011;38(5):L05704. doi:10.1029/2010GL046452.

12. Thomson AM, Calvin KV, Smith SJ, Kyle GP, Volke A, Patel P, et al. RCP4.5: a pathway for stabilization of radiative forcing by 2100. Clim Change. 2011;109(1-2):77–94.

13. Riahi K, Rao S, Krey V, Cho C, Chiniaswamy V, Guenther P, et al. RCP 8.5–A scenario of comparatively high greenhouse gas emissions. Clim Change. 2011;109(1-2):33–57.

14. Zhang X, Alexander L, Hegerl GC, Jones P, Tank AK, Peterson TC, et al. Indices for monitoring changes in extreme daily temperature and precipitation. Wiley Interdiscip Rev Clim Change. 2011;2(6):851–70. doi:10.1002/wcc.147.

15. Talchabhadel R, Karki R, Thapa BR, Maharjan M, Parajuli B. Spatiotemporal variability of rainfall-runoff of the East Rapti River basin of Nepal. Theor Appl Climatol. 2021;143(1-2):789–805. doi:10.1007/s00704-020-03451-y.

16. Shapiro SS, Wilk MB. An analysis of variance test for normality (complete samples). Biometrika. 1965;52(3/4):591–611. doi:10.1093/biomet/52.3-4.591.

17. Kolmogorov AN. On the empirical determination of a distribution law. J Ital Inst Actuaries. 1933;4:83–91.

18. Smirnov NV. Table for estimating the goodness of fit of empirical distributions. Ann Math Stat. 1948;19(2):279–81.

19. Mann HB. Nonparametric tests against trend. Econometrica. 1945;13(3):245–59. doi:10.2307/1907187.

20. Kendall MG. Rank Correlation Methods. 4th ed. London: Charles Griffin; 1975.

21. Dickey DA, Fuller WA. Distribution of the estimators for autoregressive time series with a unit root. J Am Stat Assoc. 1979;74(366a):427–31. doi:10.1080/01621459.1979.10482531.

22. Kalnay E, Kanamitsu M, Kistler R, Collins W, Deaven D, Gandin L, et al. The NCEP/NCAR 40-year reanalysis project. Bull Amer Meteorol Soc. 1996;77(3):437–71. doi:10.1175/1520-0477(1996)077<0437:TNYRP>2.0.CO;2.

23. Canadian Centre for Climate Modelling and Analysis. CCCma CanESM2 model output prepared for CMIP5 historical [Dataset]. Victoria (BC): Environment and Climate Change Canada; 2011. Available from: https://doi.org/10.1594/WDCC/CMIP5.CMACHA.

24. Nash JE, Sutcliffe JV. River flow forecasting through conceptual models part I–A discussion of principles. J Hydrol. 1970;10(3):282–90.

25. Durbin J, Watson GS. Testing for serial correlation in least squares regression. I. Biometrika. 1950;37(3-4):409-28. doi:10.1093/biomet/37.3–4.409.

26. Python Software Foundation. Python programming language, version 3.4 [Software]. 2014. Available from: https://www.python.org/.

27. Wang B, Zhang M, Wei J, et al. Changes in extreme precipitation over China in the 21st century from CMIP5 models. Theor Appl Climatol. 2016;123(1-2):395–404.

28. Mahmood R, Babel MS. Evaluation of SDSM developed by using CMIP5 GCMs for projecting temperature and precipitation in the Jhelum River basin, Pakistan and India. Theor Appl Climatol. 2014;115(3-4):389–400.

29. Alamgir M, Shahid S, Hazarika MK, et al. Analysis of meteorological drought in Bangladesh using multi-model ensemble projections. Climate. 2020;8(2):31.

30. Akinsanola AA, Ogunjobi KO. Evaluation of the simulation of present-day rainfall regime over West Africa by CMIP5 models. Earth Syst Environ. 2017;1(2):1–11.

31. Loo YY, Billa L, Singh A. Effect of climate change on seasonal monsoon in Asia and its impact on the variability of monsoon rainfall in Southeast Asia. Geosci Front. 2015;6(6):817–23.

32. Vu MT, Raghavan SV, Liu J, Liong SY. Constructing a rainstorm envelope curve for an extreme flood event in Central Vietnam under climate change. Theor Appl Climatol. 2016;126(3):611–23. doi:10.1007/s00704-015-1596-4.

33. Samadi S, Zahraee B, Taye MT, Sieber J. Statistical downscaling of river runoff in a semi-arid catchment: A case study of the Karkheh River Basin, Iran. J Arid Environ. 013;92:99–110. doi:10.1016/j.jaridenv.2013.01.011.

34. Mannig B, Müller M, Starke E, et al. Dynamical downscaling of 21st century climate change over Central Asia. Tellus A Dyn Meteorol Oceanogr. 2013;65(1):19473. doi:10.3402/tellusa.v65i0.19473.

35. Sillmann J, Kharin VV, Zhang X, Zwiers FW, Bronaugh D. Climate extremes indices in the CMIP5 multimodel ensemble: Part 2. Future climate projections. J Geophys Res Atmos. 2013;118(6):2473–93. doi:10.1002/jgrd.50188.

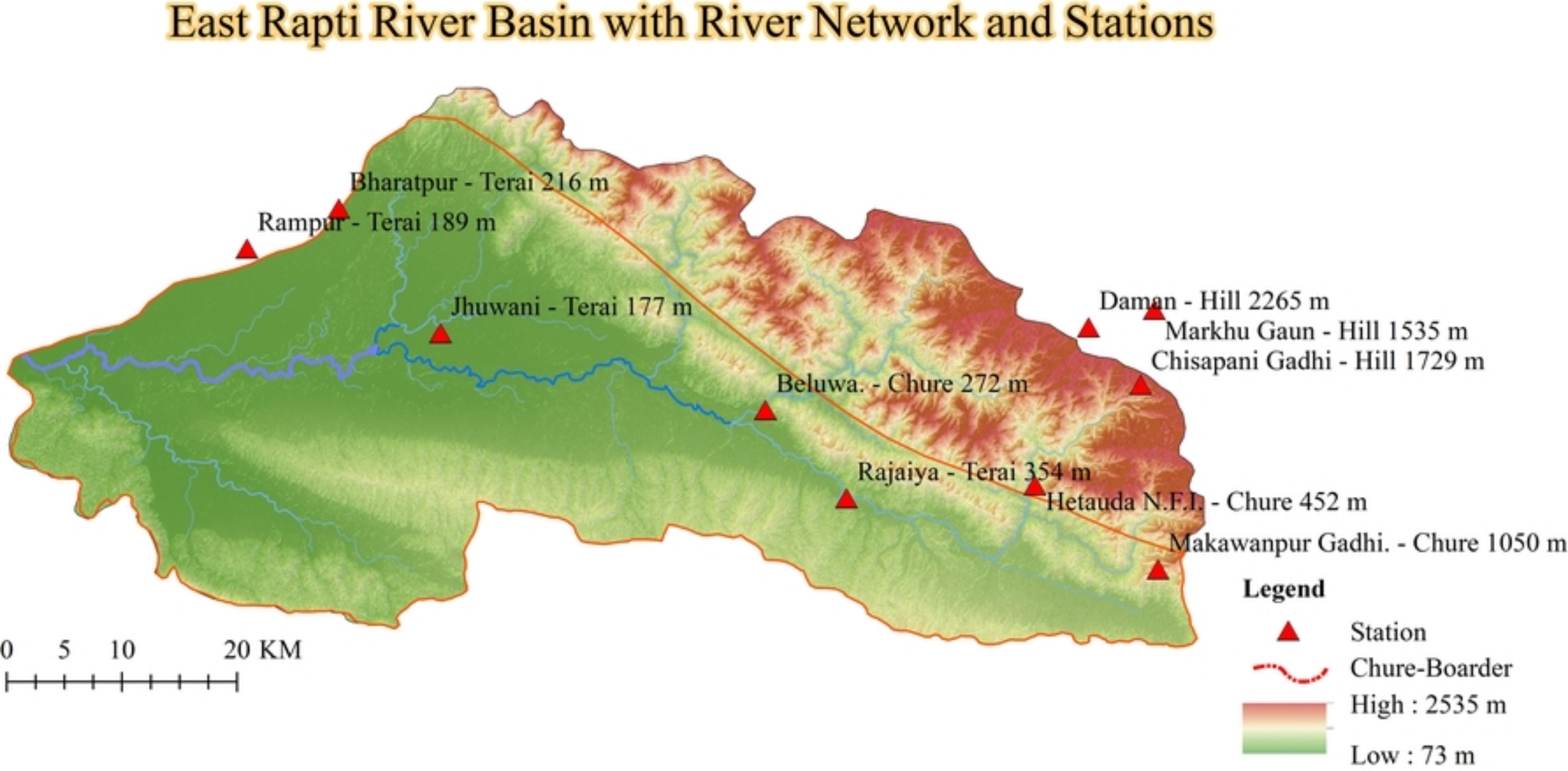
East Rapti River Basin with River Network and Stations
Bharatpur - Terai 216 m
Rampur - Terai 189 m
Jhuwani - Terai 177 m
Daman - Hill 2265 m
Markhu Gaun - Hill 1535 m
Chisapani Gadhi - Hill 1729 m
Beluwa. - Chure 272 m
Rajaiya - Terai 354 m
Hetauda N.F.I. - Chure 452 m
Makawanpur Gadhi. - Chure 1050 m
0 5 10 20 KM
Legend
Station
Chure-Boarder
High : 2535 m
Low : 73 m

Figure